Microwave spectrum, structure, and electric dipole moment of the Ar–formamide van der Waals complex

ARTICLE *in* THE JOURNAL OF CHEMICAL PHYSICS · NOVEMBER 1988

Impact Factor: 2.95 · DOI: 10.1063/1.455429

Microwave spectrum, structure, and electric dipole moment of the Ar–formamide van der Waals complex

R. D. Suenram, G. T. Fraser, F. J. Lovas, C. W. Gillies, and J. Zozom

Citation: J. Chem. Phys. **89**, 6141 (1988); doi: 10.1063/1.455429
View online: http://dx.doi.org/10.1063/1.455429
View Table of Contents: http://jcp.aip.org/resource/1/JCPSA6/v89/i10
Published by the American Institute of Physics.

Microwave spectrum, structure, and electric dipole moment of the Ar–formamide van der Waals complex

R. D. Suenram, G. T. Fraser, and F. J. Lovas
National Bureau of Standards, Molecular Spectroscopy Division, Gaithersburg, Maryland 20899

C. W. Gillies and J. Zozom
Department of Chemistry, Rensselaer Polytechnic Institute, Troy, New York 12181

(Received 29 June 1988; accepted 15 August 1988)

The microwave spectrum of the Ar–formamide van der Waals complex has been obtained using a pulsed-nozzle Fourier-transform microwave spectrometer. The rotational constants of the complex are: $A = 10\,725.7524(48)$ MHz, $B = 1771.0738(22)$ MHz, and $C = 1548.9974(16)$ MHz. The complex is shown to be nonplanar with an inertial defect of $-6.21\ u\ \text{Å}^2$. The Ar atom is located at 3.62 Å from the center of mass of the formamide unit at Ar–O, Ar–N, and Ar–C distances of 3.55, 3.79, and 3.93 Å, respectively. The shortest Ar–H distance is 3.25 Å which is similar to that observed for Ar–vinyl cyanide (3.21 Å). Stark effect and hyperfine analyses yield the following values for the electric dipole moment components and ^{14}N quadrupole coupling constants for the complex: $\mu_a = 0.922(1)$ D, $\mu_b = 3.407(5)$ D, $\chi_{aa} = -1.164(7)$ MHz, $\chi_{bb} = 1.906(5)$ MHz, and $\chi_{cc} = -0.742(6)$ MHz.

INTRODUCTION

During our investigations of the formamide–water and formamide–methanol complexes[1] by pulsed-nozzle Fourier-transform microwave spectroscopy,[2] a number of rotational transitions were observed and assigned to the Ar–formamide complex. The structure of the complex is similar to that of Ar–vinyl cyanide, which has been previously studied.[3] For Ar-vinyl cyanide, two sets of rotational transitions are observed which are assigned to two different tunneling states of the complex. The energy separation between these two states is estimated to be $\sim 0.6\ \text{cm}^{-1}$ by relative intensity measurements, using the assumption that the two tunneling states are equilibrated at the ~ 1 K rotational temperature of the expansion. The tunneling motion is assumed to involve a partial rotation of the vinyl cyanide subunit about its *a* principal axis through a transition state in which the complex has a planar configuration.

Because of the similarities between the structures of Ar–formamide and Ar–vinyl cyanide the same type of tunneling motion might also exist for Ar–formamide. For this reason, the study of Ar–formamide could be useful in gaining more detailed insights into the inversion dynamics of Ar–vinyl cyanide.

EXPERIMENTAL

A detailed description of the Fourier transform spectrometer[4] and heated-nozzle source[1] has been given elsewhere and will not be presented here. Transitions for the Ar–formamide complex, which were observed during our investigations of the H_2O–formamide and CH_3OH–formamide complexes,[1] are listed in Table I. The assignment of the lines to an Ar/formamide complex was made by noting that they required both Ar and formamide to be present for their observation. The identification of the species as a binary complex was obtained from the resulting rotational constants, quadrupole coupling constants, and electric dipole moment components which are only consistent with the dimer of Ar and formamide.

ROTATIONAL ANALYSIS

Transitions were measured for Ar–formamide between 9.1 and 16.1 GHz. A total of 15 *a*- and *b*-type lines were observed for $K_{-1} = 0$ and 1. Attempts to find *c*-type transitions were unsuccessful. The observed rotational transitions are split by the $I = 1$, ^{14}N nuclear quadrupole interaction. A sample spectrum illustrating this hyperfine splitting is shown in Fig. 1 for the 3_{12}–2_{11} transition near 10 285 MHz. The measured hyperfine lines were iteratively fit to obtain quadrupole coupling constants and rotational line centers using the usual first-order treatment of the nuclear quadrupole interaction.[5] The coupling constants determined from the fit are $\chi_{aa} = -1.164(7)$ MHz, $\chi_{bb} = 1.906(5)$ MHz, and $\chi_{cc} = -0.742(6)$ MHz. The standard deviation of the hyperfine fit is 4.9 kHz.

The line centers from the hyperfine fit, which are listed in Table I, were least squares fit to the Watson asymmetric top Hamiltonian in the I^R representation.[6] Since no $K_{-1} > 1$ transitions were observed a complete centrifugal distortion analysis was not warranted. In fact, only three of the five Watson quartic distortion constants were determined. These are Δ_J, Δ_{JK}, and δ_J. In addition to the three quartic distortion constants, we also fit a sextic distortion constant H_J. The spectroscopic constants determined from the fit are listed in Table II. The standard deviation of the fit is 8.5 kHz which is slightly larger than expected with a measurement precision of 2–4 kHz. The constants are uncorrelated, though, with the magnitude of the largest off-diagonal correlation matrix element being 0.95 between H_J and Δ_J.

The rotational constants are affected by the neglect of Δ_K and δ_K contributions to the rotational frequencies in the least squares fit. Here, Δ_K contributions will mainly affect the *A* rotational constant while δ_K contributions will mostly

TABLE I. Observed transition frequencies for Ar–formamide.

Transition $J'_{k_p k_o} - J''_{k_p k_o}$	F'–F''	Frequency (MHz)	Obs. − calc. (kHz)
1_{10}–1_{01}		9 175.802[a]	− 4.0
	1–0	9 175.029	5.4
	1–2	9 175.559	0.7
	2–2	9 175.781	0.1
	2–1	9 176.133	2.8
	0–1	9 176.464	− 0.1
2_{11}–2_{02}		9 399.987	− 7.7
	2–2	9 399.792	− 1.2
	3–3	9 400.043	0.6
	1–1	9 400.182	1.2
3_{12}–3_{03}		9 743.709	− 7.7
	3–3	9 743.429	− 3.8
	4–4	9 743.805	3.9
	2–2	9 743.930	0.0
3_{03}–2_{02}		9 941.439	− 8.8
	2–1	9 941.373	0.5
	4–3	9 941.449	0.7
4_{13}–4_{04}		10 215.775	8.5
	4–4	10 215.455	− 2.4
	5–5	10 215.896	5.5
	3–3	10 216.000	− 1.8
3_{12}–2_{11}		10 285.166	− 3.8
	3–2	10 285.091	− 4.9
	2–1	10 285.128	1.3
	4–3	10 285.207	− 5.0
6_{06}–5_{15}		12 256.884	0.7
	6–5	12 256.600	6.2
	7–6	12 256.995	− 3.8
	5–4	12 257.063	− 8.1
1_{11}–0_{00}		12 273.737	5.0
	0–1	12 272.785	1.1
	2–1	12 273.642	0.3
	1–1	12 274.209	− 4.6
7_{16}–7_{07}		12 526.480	− 1.6
	7–7	12 526.072	− 11.2
	8–8	12 526.648	4.6
	6–6	12 526.726	1.8
4_{14}–3_{13}		12 819.230	− 7.6
	4–3	12 819.206	2.2
	5–4	12 819.230	− 4.7
	3–2	12 819.261	4.1
4_{04}–3_{03}		13 233.765	− 0.4
	3–2	13 233.730	− 0.1
	5–4	13 233.754	− 13.2
	4–3	13 233.783	1.6
4_{13}–3_{12}		13 705.827	11.8
	4–3	13 705.800	0.9
	5–4	13 705.850	0.4
2_{12}–1_{01}		15 369.310	7.7
	1–0	15 368.539	− 3.4
	3–2	15 369.197	− 1.8
	1–1	15 369.426[b]	10.0
	2–2	15 369.426[b]	− 11.0
	2–1	15 369.773	− 13.6
5_{15}–4_{14}	6–5	16 013.106[b]	0.2
7_{07}–6_{16}		16 042.673	− 0.4
	7–6	16 042.419	6.4
	8–7	16 042.774	− 5.3
	6–5	16 042.832	− 2.9

[a] The first entry for each transition is the hyperfine free line center as determined from the least squares fit.

[b] This transition was not used in the hyperfine analysis because several hyperfine components are unresolved.

affect the difference, but not the sum, of the B and C rotational constants. For instance, if we fix $\Delta_K = -0.5$ MHz in the fit, the B and C rotational constants are essentially unchanged while the A rotational constant decreases by approximately 500 kHz. Alternatively, if we fix $\delta_K = -0.5$ MHz in the fit, the A and $B + C$ rotational constants change by less than 25 kHz while the $B - C$ rotational constant decreases by ~ 1.6 MHz. It should be noted that a slightly better fit of the data is obtained by including the δ_K distortion constant ($\sigma = 4.1$ kHz) directly. The resulting spectroscopic constants, though, are highly correlated, with a number of the off-diagonal correlation matrix elements having magnitudes larger than 0.99.

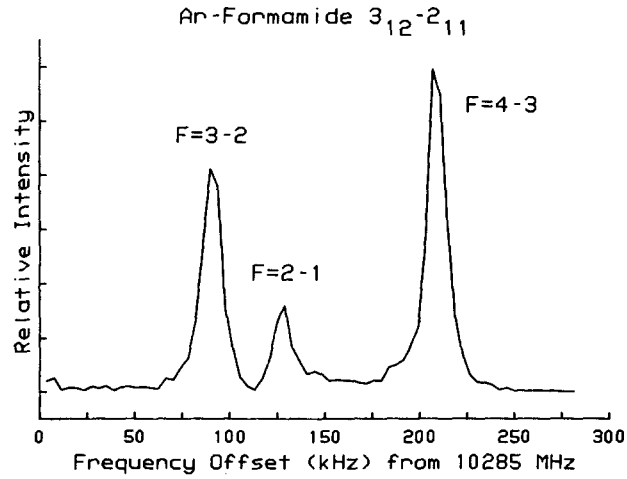

FIG. 1. Spectrum of the 3_{12}–2_{11} transition of Ar–formamide. The plot is the frequency domain spectrum obtained from the Fourier transform of the time domain result of 2000 nozzle pulses. Note we are operating in the low backing pressure region where no Doppler doubling occurs. (Ref. 4). The FWHM for these transitions is 12–14 kHz.

ELECTRIC DIPOLE MOMENT DETERMINATION

The dipole moment components μ_a and μ_b were determined by measuring the Stark effects of individual hyperfine components of the 1_{10}–1_{01}, 1_{11}–0_{00}, and 2_{12}–1_{01} transitions. These data are listed in Table III. A detailed description of the technique for measuring the Stark effect in a pulsed molecular beam Fabry–Perot spectrometer has been previously

TABLE II. Spectroscopic constants for Ar–formamide.

A	10 725.7524(48)[a]	MHz
B	1 771.0738(22)	MHz
C	1 548.9974(16)	MHz
δ_J[b]	2.8267(96)	kHz
Δ_J	22.814(67)	kHz
Δ_{JK}	468.90(33)	kHz
H_J	− 2.38(76)	Hz
σ[c]	8.5	kHz
Δ[d]	− 6.21	u Å^2
χ_{aa}	− 1.164(7)	MHz
χ_{bb}	1.906(5)	MHz
χ_{cc}	− 0.742(6)	MHz

[a] Experimental uncertainties are one standard error from the least squares fit.

[b] The other two quartic distortion constants (δ_k and Δ_k) were constrained to zero in the least squares fit.

[c] Standard deviation of the least squares fit to determine the rotation and distortion constants.

[d] Inertial defect ($\Delta \equiv I_{cc} - I_{bb} - I_{aa}$).

TABLE III. Stark effect measurements on the 1_{10}–1_{01}, 1_{11}–0_{00}, and 2_{12}–1_{01} transitions of Ar–formamide.

	F'	F''	$\lvert M_F\rvert$	E(V/cm)[a]	ν(MHz)	Obs. − calc.(kHz)[b]
1_{10}–1_{01}	1	0	0	7.684	9 175.052	− 5.5
				15.367	9 175.120	− 6.4
				23.051	9 175.236	− 4.8
				30.735	9 175.394	− 5.9
1_{10}–1_{01}	0	1	0	7.684	9 176.481	− 1.7
				15.367	9 176.540	− 1.1
				23.051	9 176.644	− 1.8
				30.735	9 176.804	1.9
1_{11}–0_{00}	2	1	0	30.735	12 273.786	− 3.8
				38.419	12 273.888	− 0.8
				40.724	12 273.925	0.4
				53.786	12 274.185	1.4
1_{11}–0_{00}	2	1	1	30.735	12 273.669	− 2.9
				38.419	12 273.657	− 3.2
				40.734	12 273.649	− 4.1
				53.786	12 273.575	− 5.7
				61.470	12 273.510	− 4.5
1_{11}–0_{00}	1	1	1	30.735	12 274.414	− 5.5
				46.102	12 274.545	− 3.7
				53.786	12 274.707	− 7.6
1_{11}–0_{00}	0	1	0	38.419	12 272.763	1.6
				47.639	12 272.721	− 0.1
				57.628	12 272.654	1.3
				65.312	12 272.584	1.5
				76.837	12 272.455	4.8
2_{12}–1_{01}	1	0	0	30.735	15 368.432	− 7.6
				38.419	15 368.373	− 5.8
				57.628	15 368.143	− 6.6
				76.837	15 367.780	− 8.1

[a] Electric field known to 0.05%.
[b] Observed − calculated frequencies from the least squares fit.

given[7] so only a brief description will be presented here. A set of parallel plates were used to apply an electric field to the molecules in the cavity. The plates were 25 cm square and were spaced by 26 cm. One plate was energized with a (+) dc voltage and the other with a (−) dc voltage so that the electric field was symmetric with respect to ground at the center of the cavity. Electric fields as large as 76.8 V/cm were used, yielding the field-induced frequency shifts as much as 759 kHz. The electric field was calibrated using the Stark effect of OCS for which $\mu = 0.715\ 19(3)$ D.[8] The data were analyzed by standard methods[9] using the following Hamiltonian:

$$H = H_{\rm rot} + H_{\rm quad} - \boldsymbol{\mu}\cdot\mathbf{E}, \qquad (1)$$

where $H_{\rm rot}$ is the rotational Hamiltonian (with rotational and distortion constants of Table II), $H_{\rm quad}$ is the nuclear quadrupole interaction (with quadrupole coupling constants of Table II), μ is the electric dipole moment, and E is the electric field. Matrix elements of H were determined in the uncoupled basis $|J_{KpKo}M_J\rangle|IM_I\rangle$ where $|J_{KpKo}M_J\rangle$ are the symmetric-top wave functions which diagonalize $H_{\rm rot}$. H was effectively made diagonal in J_{KpKo} by treating the $-\boldsymbol{\mu}\cdot\mathbf{E}$ term by second-order perturbation theory. The resulting Stark-hyperfine matrices have off-diagonal elements only in M_J and M_I. Diagonalization of these matrices yields energies, and thus transition frequencies, which are least squares fit to the observed transitions by iteratively varying μ_a and μ_b. The results are shown in Table IV and the residuals from the fit are shown in Table III. The standard deviation of the fit is 4.6 kHz. A nonzero value for μ_c only decreases the quality of the fit. For example, if we fix μ_c at 0.50 D in the fit then the standard deviation increases to 6.7 kHz while μ_a and μ_b remain essentially unchanged, as shown in Table IV.

TABLE IV. Electric dipole moments components (in Debye) for Ar–formamide.

	Observed		Calculated[a]	
			I,IV[b]	II,III[b]
μ_a	0.922(1)[c]	0.928(2)	1.034	0.232
μ_b	3.407(5)	3.403(7)	3.518	3.669
μ_c	0[d]	0.5[d]	0.594	0.536

[a] Calculated from structures I–IV by projecting the μ_a and μ_b components of formamide onto the principal axes of the complex. See the text for discussion.
[b] For structure *I*, $\theta = 84.6°$, $\phi = 42.3°$; for structure *II*, $\theta = 84.6°$, $\phi = 222.3°$; for structure *III*, $\theta = 95.4°$, $\phi = 317.7°$; for structure *IV*, $\theta = 95.4°$, $\phi = 137.7°$.
[c] The numbers in parentheses represent one standard error from the least squares fit.
[d] Fixed at this value. See the text for discussion.

The large inertial defect for Ar–formamide, $\Delta = -6.21\ u\ \text{Å}^2$, is inconsistent with a planar complex, implying that μ_c must be nonzero. Despite this, attempts to observe the 1_{10}–0_{00} and the 2_{11}–1_{01} ($\sim$12 500 and 16 040, respectively) *c*-type transitions at the frequencies predicted from the asymmetric top analysis of the *a*- and *b*-type spectrum have been unsuccessful. One possibility is that the complex is nonrigid resulting in *c*-type selection rules which are not pure rotation, but rather rotation–inversion, so that the *c*-type transitions are not detected at their expected rigid rotor frequencies but are shifted by the inversion frequency. The *a*- and *b*-type transitions, which follow pure-rotation selection rules, take place entirely within the symmetric tunneling state while the *c*-type transitions occur between the symmetric and antisymmetric tunneling states. For a sufficiently large tunneling splitting the antisymmetric tunneling state would not be expected to be populated at the 1 K rotational temperature of the expansion so that no transitions would be observed within this state. In addition, a large tunneling splitting will shift the frequencies of the *c*-type rotation–inversion lines outside the frequency range of the Fourier transform microwave spectrometer, preventing their observation. The presence of a *c*-type rotation–inversion spectrum could explain the systematic negative residuals obtained in the Stark analysis (Table III) since here we have considered only *c*-type Stark connections which follow the rigid rotor pattern constructed from the *a*- and *b*-type transitions.

STRUCTURAL ANALYSIS

In the structural analysis we will assume that the geometry of formamide[10] is unchanged by complexation with Ar. Within this approximation, there are three coordinates necessary to specify the structure of Ar–formamide. These are conveniently taken as the polar coordinates shown in Fig. 2. The polar coordinate system is referenced to the principal

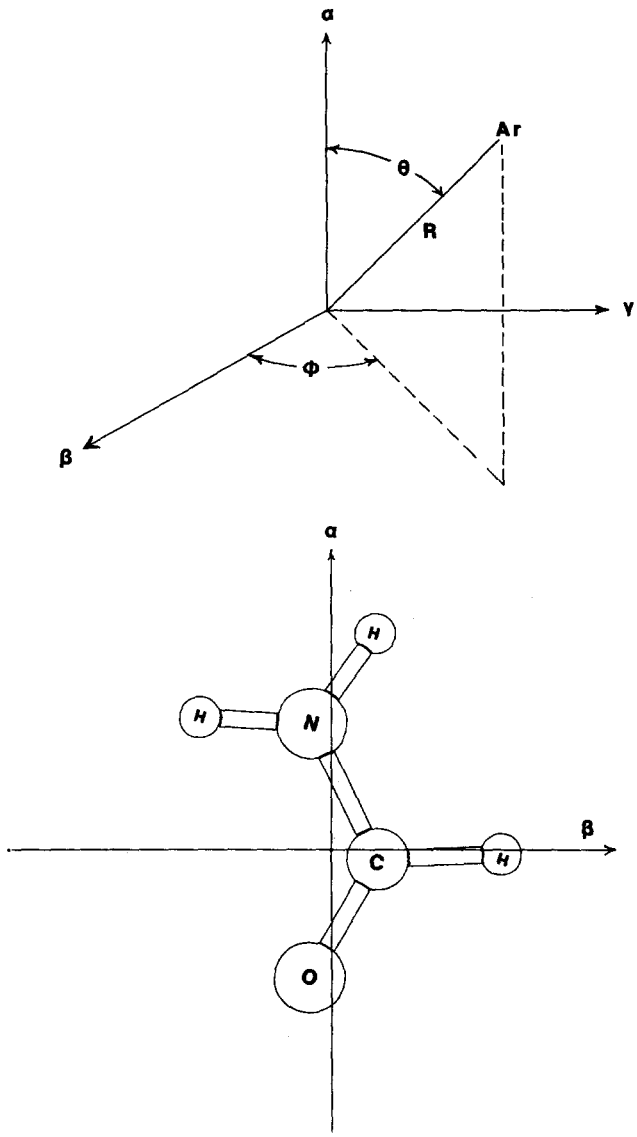

FIG. 2. Polar coordinate system used to discuss the structure of Ar–formamide. The α, β, and γ axes refer to the *a*,*b*, and *c* axes of formamide.

axes of inertia of formamide. In the figure α, β, and γ refer to the *a b*, and *c* principal axes of formamide. The polar coordinates are: R, the distance between the center of mass of formamide and Ar; θ, the angle between a vector along R and the α axis of formamide; and ϕ, the angle between the β axis of formamide and the protection of R onto the β–γ plane.

The inertia tensor of the complex, in the center-of-mass frame, can be expressed in terms of R, θ, and ϕ. The center-of-mass axis system, which differs from the (β,γ,α) axis system by a translation, will be designated (x,y,z). The components of the inertia tensor in the (x,y,z) frame are

$$\begin{aligned} I_{zz} &= I^f_{\alpha\alpha} + \mu R^2 \sin^2\theta, \\ I_{xx} &= I^f_{\beta\beta} + \mu R^2(\cos^2\theta + \sin^2\theta \sin^2\phi), \\ I_{yy} &= I^f_{\gamma\gamma} + \mu R^2(\cos^2\theta + \sin^2\theta \cos^2\phi), \\ I_{zx} &= -\mu R^2 \cos\theta \sin\theta \cos\phi, \\ I_{zy} &= -\mu R^2 \cos\theta \sin\theta \sin\phi, \\ I_{xy} &= -\mu R^2 \sin^2\theta \sin\phi \cos\phi, \end{aligned} \tag{2}$$

where $I^f_{\alpha\alpha}$, $I^f_{\beta\beta}$, and $I^f_{\gamma\gamma}$ are the moments of inertia of formamide, and μ is the pseudodiatomic reduced mass of the complex. Diagonalization of the inertia tensor yields moments of inertia and thus rotational constants for the complex.

For Ar–formamide of C_1 symmetry there are four sets of the (R,θ,ϕ) coordinates which give different structures for the complex but still yield rotational constants in agreement with experiment. This results since the inertia tensor of the complex is invariant to a 180° rotation of the formamide unit about any of its principal axes. The sets of coordinates which reproduce the observed rotational constants are (R_0,θ_0,ϕ_0), $(R_0,\theta_0,\pi+\phi_0)$, $(R_0,\pi-\theta_0,\ 2\pi-\phi_0)$, and $(R_0,\pi-\theta_0,\ \pi-\phi_0)$ where $R_0 = 3.624$ Å, $\theta_0 = 84.6°$, and $\phi_0 = 42.3°$. The corresponding structures will be designated I, II, III, and IV, respectively.

Two of the four structural possibilities can be eliminated by considering the electric dipole moment measurements for the complex. In Table IV we compare the experimental dipole moment components with those predicted for structures I–IV by projecting the dipole moment of formamide ($\mu_\alpha = 3.616$ D and $\mu_\beta = 0.852$ D[11]) onto the inertial axes of the complex. Here, we have assumed that the induced dipole moments which arise from complexation are negligible. This is reasonable since for Ar complexes they are typically < 0.3 D.[12–16] As seen in the Table, structures II and III can be rejected since the estimated μ_a values for these structures are in poor agreement with experiment.

In order to rule out one of the two remaining structures, we can examine the nearest neighbor distances predicted for these two structural possibilities. For structure I, the shortest Ar–H distance is 2.72 Å while for structure IV it is 3.25 Å. Ar–H van der Waals distances vary from the 2.63 Å observed in Ar–HF[17] to the 3.41 Å observed in Ar–CH_3Cl.[18] Since formamide is not nearly as acidic as HF, or for that matter HCl, the Ar–H distance in Ar–formamide is not expected to be close to that of Ar–HF or even Ar–HCl (2.73 Å).[19] Because of this, the 3.25 Å distance and its corresponding structure (IV) seem most reasonable. We note that the 3.25 Å separation in Ar–formamide is close to the 3.33 Ar–H distance observed in $Ar(HCN)_2$.[20] Structure IV, which has $R = 3.624$ Å, $\theta = 95.4°$, and $\phi = 137.7°$ in Fig. 2, is shown in Fig. 3. For structure IV the Ar–O, Ar–N, and Ar–C distances are 3.55, 3.79, and 3.93 Å, respectively.

Structural information is also available from the measured quadrupole coupling constants of Ar–formamide since the coupling constants of the complex are determined from the vibrationally averaged projections of the coupling constants of formamide onto the inertial axes of the complex. This is true if we assume that the electric field gradient at the nitrogen nucleus is unaffected by complexation. For Ar–formamide, modeling of the quadrupole coupling constants of the complex is difficult because we do not know all the components of the quadrupole tensor of formamide. The diagonal components of the tensor have been determined by Kukolich and Nelson using microwave spectroscopy and are $\chi_{\alpha\alpha} = 1.960(2)$ MHz, $\chi_{\beta\beta} = 1.888(3)$ MHz, and $\chi_{\gamma\gamma} = -3.848(4)$ MHz.[21] Two of the off-diagonal components, $\chi_{\alpha\gamma}$ and $\chi_{\beta\gamma}$ are zero by symmetry. The remaining off-diagonal component, $\chi_{\alpha\beta}$, is not zero by symmetry and has not been measured.

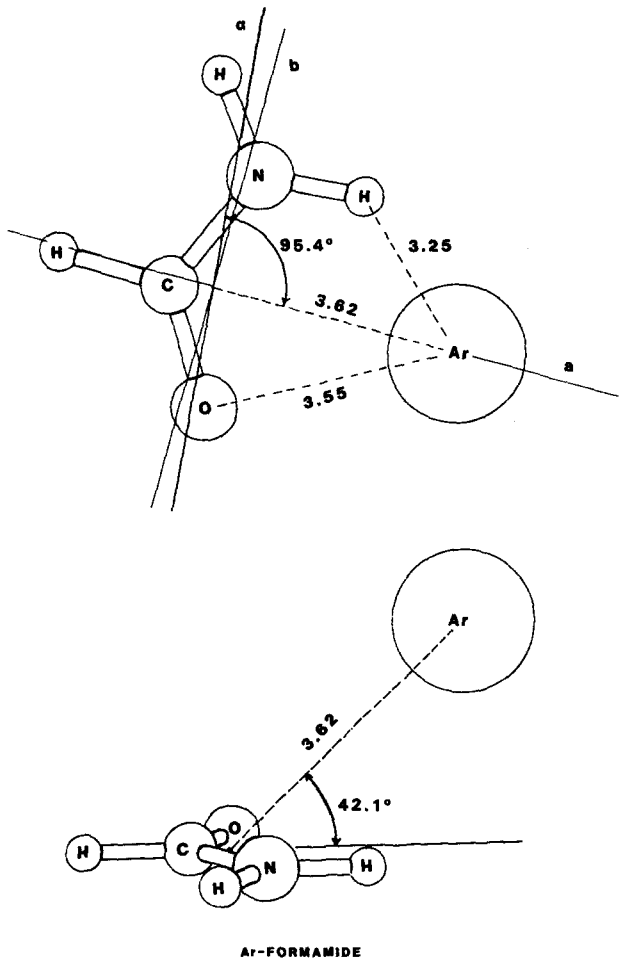

FIG. 3. Structure of the Ar–formamide van der Waals complex. Here $R = 3.624$ Å, $\theta = 95.4°$, and $\phi = 137.7°$. The a and b axes are the principal axes of the complex and α is the a principal axis of the formamide monomer. In the lower figure 42.1° is the angle to project R onto the α–β plane (i.e., $\arcsin[\sin\theta \sin\phi]$).

As discussed by Kurland and Wilson[10] for formamide, an idealized set of sp^2-hybridized nitrogen orbitals gives a field gradient at the nitrogen nucleus which is cylindrically symmetric about an axis perpendicular to the plane of formamide. This implies that $\chi_{\alpha\beta} = 0$ and $\chi_{\alpha\alpha} = \chi_{\beta\beta}$. Since the measurements of Kukolich and Nelson[21] show that $\chi_{\alpha\alpha} \simeq \chi_{\beta\beta}$, we will assume that $\chi_{\alpha\beta} \simeq 0$. Taking $\chi_{\alpha\alpha} = 1.960$ MHz, $\chi_{\beta\beta} = 1.888$ MHz, and $\chi_{\gamma\gamma} = -3.848$ MHz, and using the rotation matrix which diagonalizes the inertia tensor of Eq. (2), we find that for structures I–IV of Ar–formamide: $\chi_{aa} = -0.609$ MHz, $\chi_{bb} = 1.933$ MHz, and $\chi_{cc} = -1.324$ MHz. These results are in poor agreement with the experimentally determined values of Table II. On the other hand, if we choose $\theta_0 = 83.15°$ and $\phi_0 = 48.17°$ with R_0 as above, we obtain coupling constants in agreement with the experimentally determined values. For structure IV this implies $\theta = 96.9°$, and $\phi = 131.8°$ compared to the rotational-constant-determined values of $\theta = 95.4°$, and $\phi = 137.7°$.

If we had not assumed that $\chi_{\alpha\beta} = 0$, we find for $|\chi_{\alpha\beta}| < 0.5$ MHz that the coupling-constant-determined values for θ and ϕ change by less than $\sim 6°$ and $\sim 1°$, respectively, from the $\chi_{\alpha\beta} = 0$ results. This implies that the 5.9° discrepancy between the coupling-constant-determined and rotational-constant-determined ϕ is not a consequence of the assumption that $x_{\alpha\beta} = 0$. It is also, most likely, not caused by complexation-induced changes in the electric-field gradient at the N nucleus for formamide since these effects have been shown to be small for rare-gas binding partners.[22,23] It may originate in differences in zero-point averaging on the coupling-constant-determined and the rotational-constant-determined values of ϕ. These effects, which have been ignored here, become important when the amplitude of the zero-point motion is large. Zero-point effects are expected to be more important for the ϕ coordinate than for the θ coordinate since the reduced mass for ϕ motion is $\sim I_{\alpha\alpha}$. $I_{\alpha\alpha}$ is a factor of 6 to 7 smaller than $I_{\beta\beta}$ and $I_{\gamma\gamma}$, which are related to the reduced mass for θ motion. Other results also point to large amplitude motion involving the ϕ coordinate, including the large negative inertial defect and the absence of c-type transitions, as well as the similarities in structures between the Ar–formamide and the nonrigid Ar–vinyl cyanide complexes.

DISCUSSION

The structure of Ar–formamide (Fig. 3) is similar to that of Ar–vinyl cyanide[3] and Ar-vinyl chloride.[24] No c-type transitions are observed for each of these nonplanar complexes at the expected rigid rotor frequencies. This implies that the c-type transitions do not follow pure rotational selection rules but rather rotation–inversion selection rules. For Ar–formamide only one set of rotational states is observed and these are assigned to the symmetric tunneling state. For both Ar–vinyl cyanide and Ar–vinyl chloride two sets of rotational transitions are observed—one set for the symmetric tunneling state and one set for the antisymmetric tunneling state.

The observation of only one set of rotational transitions for Ar–formamide suggests that the tunneling frequency in Ar–formamide must be substantially larger than that of either the vinyl cyanide or vinyl chloride complex so that the antisymmetric tunneling state of Ar–formamide is not appreciably populated at the ~ 1 K rotational temperature of the molecular beam. Attempts to model the state distribution in the expansion to estimate a lower bound for the tunneling frequency in Ar–formamide is made difficult since rotational and vibrational degrees of freedom are not equilibrated in the expansion.

Presently, the most likely model for the tunneling motion consists of a partial rotation of the formamide subunit around its α-inertial axis through a planar configuration of the complex. The a and b dipole moment components of the complex would be symmetric with respect to this motion while the c dipole moment component would be antisymmetric. This picture could be verified by the observation of c-type rotation–inversion transitions. Attempts to observe these lines have so far been unsuccessful for Ar–formamide, Ar–vinyl chloride and Ar–vinyl cyanide, due to the difficulty of estimating the tunneling frequency, and due to the possibility that the optimum rotation–inversion transitions are outside the frequency coverage of the spectrometer.

[1]F. J. Lovas, R. D. Suenram, G. T. Fraser, C. W. Gillies, and J. Zozom, J. Chem. Phys. **88**, 722 (1988).
[2]T. J. Balle and W. H. Flygare, Rev. Sci. Instrum. **52**, 33 (1981).
[3]R. D. Suenram and F. J. Lovas, J. Chem. Phys. **87**, 4447 (1987).
[4]F. J. Lovas and R. D. Suenram, J. Chem. Phys. **87**, 2010 (1987).
[5]C. H. Townes and A. L. Schawlow, *Microwave Spectroscopy* (Dover, New York, 1975).
[6]J. K. G. Watson, J. Chem. Phys. **46**, 1935 (1967).
[7]L. H. Coudert, F. J. Lovas, R. D. Suenram, and J. T. Hougen, J. Chem. Phys. **87**, 6290 (1987).
[8]J. M. L. J. Reinhartz and A. Dymanus, Chem. Phys. Lett. **24**, 346 (1974).
[9]W. Gordy and R. L. Cook, *Microwave Molecular Spectra* (Wiley, New York, 1970).
[10]E. Hirota, R. Sugisaki, C. J. Nielsen, and G. O. Sørensen, J. Mol. Spectrosc. **49**, 251 (1974).
[11]R. J. Kurland and E. B. Wilson, Jr., J. Chem. Phys. **27**, 585 (1957).
[12]J. M. Steed, T. A. Dixon, and W. Klemperer, J. Chem. Phys. **70**, 4095 (1979).
[13]K. C. Janda, L. S. Bernstein, J. M. Steed, S. E. Novick, and W. Klemperer, J. Am. Chem. Soc. **100**, 8074 (1978).
[14]W. L. Ebenstein and J. S. Muenter, J. Chem. Phys. **80**, 1417 (1984).
[15]R. L. DeLeon and J. S. Muenter, J. Chem. Phys. **72**, 6020 (1980).
[16]K. H. Bowen, K. R. Leopold, K. V. Chance, and W. Klemperer, J. Chem. Phys. **73**, 137 (1980).
[17]S. J. Harris, S. E. Novick, and W. Klemperer, J. Chem. Phys. **60**, 3208 (1974).
[18]G. T. Fraser, R. D. Suenram, and F. J. Lovas, J. Chem. Phys. **86**, 3107 (1987).
[19]S. E. Novick, P. Davies, S. J. Harris, and W. Klemperer, J. Chem. Phys. **59**, 2273 (1973).
[20]R. S. Ruoff, T. I. Emilsson, T. D. Klots, C. Chuang, and H. S. Gutowski, J. Chem. Phys. **88**, 1557 (1988).
[21]S. G. Kukolich and A. C. Nelson, Chem. Phys. Lett. **11**, 383 (1971).
[22]W. G. Read, E. J. Campbell, and G. Henderson, J. Chem. Phys. **78**, 3501 (1983).
[23]G. T. Fraser, R. D. Suenram, and F. J. Lovas, J. Chem. Phys. **86**, 3107 (1987).
[24]F. J. Lovas (private communication).